Computers and Mathematics with Applications 175 (2024) 224–235

Contents lists available at ScienceDirect

Computers and Mathematics with Applications

journal homepage: www.elsevier.com/locate/camwa

Convergence analysis of novel discontinuous Galerkin methods for a convection dominated problem

Satyajith Bommana Boyana [a,1], Thomas Lewis [a], Sijing Liu [b,*,2], Yi Zhang [a]

[a] Department of Mathematics and Statistics, University of North Carolina Greensboro, Greensboro, NC, USA
[b] The Institute for Computational and Experimental Research in Mathematics, Brown University, Providence, RI, USA

ARTICLE INFO

Keywords:
Discontinuous Galerkin finite element differential calculus
Dual-wind discontinuous Galerkin methods
Convection-dominated problem

ABSTRACT

In this paper, we propose and analyze a numerically stable and convergent scheme for a convection-diffusion-reaction equation in the convection-dominated regime. Discontinuous Galerkin (DG) methods are considered since standard finite element methods for the convection-dominated equation cause spurious oscillations. We choose to follow a DG finite element differential calculus framework introduced in Feng et al. (2016) and approximate the infinite-dimensional operators in the equation with the finite-dimensional DG differential operators. Specifically, we construct the numerical method by using the dual-wind discontinuous Galerkin (DWDG) formulation for the diffusive term and the average discrete gradient operator for the convective term along with standard DG stabilization. We prove that the method converges optimally in the convection-dominated regime. Numerical results are provided to support the theoretical findings.

1. Introduction

Let Ω be a convex polygonal domain in $\mathbb{R}^2$. We consider the following convection-diffusion-reaction equation

$$-\varepsilon\Delta u+\boldsymbol{\zeta}\cdot\nabla u+\gamma u=f \quad \text{in} \quad \Omega, \tag{1.1a}$$

$$u=g \quad \text{on} \quad \partial\Omega, \tag{1.1b}$$

where the diffusive coefficient $\varepsilon>0$, the source term $f\in L_2(\Omega)$, the convective velocity $\boldsymbol{\zeta}\in[W^{1,\infty}(\Omega)]^2$ and the reaction coefficient $\gamma\in W^{1,\infty}(\Omega)$ is nonnegative. We assume

$$\gamma-\frac{1}{2}\nabla\cdot\boldsymbol{\zeta}\geq\gamma_0>0 \tag{1.2}$$

for some constant γ_0 so that the problem (1.1) is well-posed. Note that the convective term in (1.1) is written in non-conservative form. It is equivalent to consider the conservative form

$$-\varepsilon\Delta u+\nabla\cdot(\boldsymbol{\zeta}u)+(\gamma-\nabla\cdot\boldsymbol{\zeta})u=f \quad \text{in} \quad \Omega, \tag{1.3a}$$

$$u=g \quad \text{on} \quad \partial\Omega. \tag{1.3b}$$

The equation (1.1)/(1.3) and the corresponding numerical methods were intensively studied in the literature [30,15,24,33,29,17,31,28,9,25] and the references therein. The difficulties of designing numerical methods to solve (1.1)/(1.3) arise when one considers the convection-dominated case, namely, when $0<\varepsilon\ll 1$. In the convection-dominated regime, the solution to (1.1) exhibits boundary layers near the outflow boundary. We refer to [30] for more discussion about the analytic behavior of the solution to (1.1). The sharp gradients in the boundary layer pose challenges in designing robust numerical methods for (1.1). It is well known that a standard finite element method for (1.1) produces spurious oscillations near the outflow boundary when $\varepsilon\leq h\|\boldsymbol{\zeta}\|_\infty$, where h is the mesh size of the triangulation. These oscillations then propagate into the interior of the domain where the solution is smooth and destroy the convergence of the finite element methods.

To remedy this issue, many methods were proposed to stabilize the numerical solutions to (1.1), for example, SUPG [5,16], local projection [14,19,20], EAFE [33,32,18] and DG methods [1,13,12,4]. We refer to [30,17,29,9] and the references therein for more details about stabilization techniques. Among these methods, discontinuous Galerkin (DG) methods are favorable in many aspects. First, DG methods do not require the numerical solutions to be continuous, and, hence, they are more suit-

* Corresponding author.
E-mail addresses: s_bomman@uncg.edu, sbommanaboyana@floridapoly.edu (S.B. Boyana), tllewis3@uncg.edu (T. Lewis), sijing_liu@brown.edu, sliu13@wpi.edu (S. Liu), y_zhang7@uncg.edu (Y. Zhang).
[1] Current address: Department of Applied Mathematics, Florida Polytechnic University, Lakeland, FL. USA.
[2] Current address: Department of Mathematical Sciences, Worcester Polytechnic Institute, Worcester, MA, USA.

https://doi.org/10.1016/j.camwa.2024.09.027
Received 9 April 2024; Received in revised form 12 August 2024; Accepted 26 September 2024

able to capture sharp gradients in the solutions. Secondly, DG methods impose the boundary conditions weakly which prevents the boundary layers propagating into the interior of the domain. Lastly, DG methods have a natural upwind stabilization that can stabilize oscillatory behaviors of the numerical solutions [1,24].

In this work, we consider a new type of DG methods inspired by the DG finite element differential calculus framework [10], to solve (1.1). Specifically, the diffusion part of the equation is discretized by the dual-wind discontinuous Galerkin (DWDG) method and the convection part is discretized by an average discrete divergence operator. DWDG methods were introduced for diffusion problems in [21] based on the DG differential calculus framework [10]. Such methods have optimal convergence properties even in the absence of a penalty term which is different from many existing DG methods. DWDG methods also have been applied to other problems [23,22,2,11]. However, the study of the DG finite element differential calculus for convection-diffusion-reaction equations is still missing in the literature. In this paper, we extend the methods to convection-diffusion-reaction equations, with a particular focus on the convection-dominated regime. In order to apply the methods, we first consider a reduced problem by taking $\varepsilon = 0$ in (1.3) and approximate the divergence operator $\nabla\cdot$ with the discrete divergence operator $\overline{\mathrm{div}}_h$. We show, with this choice of discrete operator, the method for the reduced problem is consistent with a centered fluxes DG method [7] for the convective term. This is due to the fact that the discrete operator $\overline{\mathrm{div}}_h$ is defined as the average of the "left" discrete divergence operator and the "right" discrete divergence operator. Using this equivalence, we add a standard penalty term to stabilize the numerical solution which leads to an upwind DG method. Combining the existing DWDG analysis for the diffusive equation with the aforementioned equivalence, we show that the proposed methods are optimal for the convection-diffusion-reaction equations in the sense of the following,

$$\|u - u_h\|_{h\sharp} \leq \begin{cases} O(h) & \text{if diffusion-dominated,} \\ O(h^{\frac{3}{2}}) & \text{if convection-dominated,} \end{cases} \tag{1.4}$$

where u is the solution to (1.1), u_h is the numerical solution, and the mesh-dependent norm $\|\cdot\|_{h\sharp}$ is defined in Section 4. We analyze the numerical methods using a coercive framework as well as an inf-sup approach. The inf-sup approach allows us to establish a stronger result which also controls the convective derivative (cf. [7]).

The rest of the paper is organized as follows. In Section 2, we recall the results about the DG differential calculus framework and define various discrete operators that are useful in the following sections. In Section 3, we consider the reduced problem when taking $\varepsilon = 0$. We propose the numerical approximations for the reduced problem and establish concrete error estimates. In Section 4, we propose fully discretized methods for (1.3) and justify the main convergence theorem. Finally, we provide some numerical results in Section 5 and end with some concluding remarks in Section 6.

Throughout this paper, we use C (with or without subscripts) to denote a generic positive constant that is independent of any mesh parameter. Also to avoid the proliferation of constants, we use the notation $A \lesssim B$ (or $A \gtrsim B$) to represent $A \leq (\text{constant})B$. The notation $A \approx B$ is equivalent to $A \lesssim B$ and $B \lesssim A$.

2. Notations and the DG differential calculus

In this section, we briefly introduce the DG differential calculus framework (cf. [10]) and the notations that will be used in the rest of the paper. We also provide some useful properties of the DG operators. Throughout the paper we will follow the standard notation for differential operators, function spaces, and norms that can be found, for example, in [3,6].

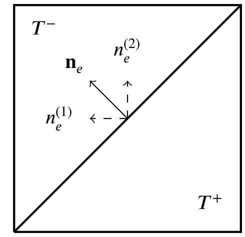

Fig. 1. The operators $Q_i^{\pm}$.

2.1. DG operators

Let $W^{m,p}(\Omega)$ denote the set of all functions that are in $L^p(\Omega)$ whose weak derivatives up to order m also belong to $L^p(\Omega)$. We denote $H^m(\Omega) := W^{m,2}(\Omega)$ when $p = 2$. Let $W_0^{m,p}(\Omega)$ be the set of functions in $W^{m,p}(\Omega)$ with vanishing traces up to order $m-1$ on $\partial\Omega$, and let $H_0^m(\Omega) = W_0^{m,2}(\Omega)$.

Let $\mathcal{T}_h$ denote a locally quasi-uniform simplicial triangulation of $\Omega \subset \mathbb{R}^2$ with a mesh size $h := \max_{T\in\mathcal{T}_h} h_T$, where h_T is the diameter of the simplex $T \in \mathcal{T}_h$. Let $\mathcal{E}_h := \bigcup_{T\in\mathcal{T}_h} \partial T$ be the set of all edges in $\mathcal{T}_h$ and $\mathcal{E}_h^B := \bigcup_{T\in\mathcal{T}_h} (\partial T \cap \partial\Omega)$ be the set of boundary edges in $\mathcal{T}_h$. Moreover, denote $\mathcal{E}_h^I := \mathcal{E}_h \setminus \mathcal{E}_h^B$ as the set of interior edges in $\mathcal{T}_h$. We now define the following piecewise Sobolev spaces

$$W^{m,p}(\mathcal{T}_h) := \{v : v|_T \in W^{m,p}(T) \quad \forall\, T \in \mathcal{T}_h\},$$

$$\boldsymbol{W}^{m,p}(\mathcal{T}_h) := \{\boldsymbol{v} : \boldsymbol{v}|_T \in W^{m,p}(T) \times W^{m,p}(T) \quad \forall\, T \in \mathcal{T}_h\}.$$

We then denote

$$\mathcal{V}_h := W^{1,1}(\mathcal{T}_h) \cap C^0(\mathcal{T}_h) \quad \text{and} \quad \boldsymbol{\mathcal{V}}_h := \mathcal{V}_h \times \mathcal{V}_h. \tag{2.1}$$

We also define the following inner products,

$$(v, w)_{\mathcal{T}_h} := \sum_{T\in\mathcal{T}_h} \int_T v w\, dx \quad \text{and} \quad \langle v, w\rangle_{\mathcal{S}_h} := \sum_{e\in\mathcal{S}_h} \int_e v w\, ds, \tag{2.2}$$

where $\mathcal{S}_h$ is a subset of $\mathcal{E}_h$.

Define the DG space

$$V_h := \{v \in L_2(\Omega) : v|_T \in \mathbb{P}_1(T) \quad \forall\, T \in \mathcal{T}_h\} \tag{2.3}$$

and define $\boldsymbol{V}_h := V_h \times V_h$. Note that $V_h \subset \mathcal{V}_h$ and $\boldsymbol{V}_h \subset \boldsymbol{\mathcal{V}}_h$. For each edge $e = \partial T^+ \cap \partial T^-$ with some T^+ and T^- in $\mathcal{T}_h$, we assume the global numbering of T^+ is more than that of T^- for simplicity. We define the jump and the average across an edge $e \in \mathcal{E}_h^I$ as follows:

$$[v]|_e := v^+ - v^-, \qquad \{v\}|_e := \frac{1}{2}\left(v^+ + v^-\right) \qquad \forall\, v \in \mathcal{V}_h,$$

where $v^{\pm} := v|_{T^{\pm}}$. If an edge $e \in \mathcal{E}_h^B$, then define

$$[v]|_e := v^+, \qquad \{v\}|_e := v^+ \qquad \forall\, v \in \mathcal{V}_h.$$

For an edge $e \in \mathcal{E}_h^I$, set $\mathbf{n}_e = (n_e^{(1)}, n_e^{(2)})^t := \mathbf{n}_{T^+}|_e = -\mathbf{n}_{T^-}|_e$ as the unit normal vector. Given any $v \in \mathcal{V}_h$, the trace operator $Q_i^{\pm}$ on $e \in \mathcal{E}_h^I$ in the direction x_i $(i = 1, 2)$ is defined as follows:

$$Q_i^+(v) := \begin{cases} v|_{T^+}, & n_e^{(i)} > 0 \\ v|_{T^-}, & n_e^{(i)} < 0 \\ \{v\}, & n_e^{(i)} = 0 \end{cases} \quad \text{and} \quad Q_i^-(v) := \begin{cases} v|_{T^-}, & n_e^{(i)} > 0 \\ v|_{T^+}, & n_e^{(i)} < 0 \\ \{v\}, & n_e^{(i)} = 0 \end{cases}.$$

See Fig. 1 for an example where $Q_1^+(v) = v|_{T^-}$ and $Q_2^-(v) = v|_{T^+}$. Alternatively, we can define $Q_i^{\pm}(v) := \{v\} \pm \frac{1}{2}\mathrm{sgn}(n_e^{(i)})[v]$, and hence the operators $Q_i^+(v)$ and $Q_i^-(v)$ can be interpreted as "right" and "left" limits in the x_i direction on $e \in \mathcal{E}_h^I$. For $e = \partial T^+ \cap \partial\Omega \in \mathcal{E}_h^B$, we simply set $Q_i^{\pm}(v) := v^+$.

Having defined the trace operators as above, for any $v \in \mathcal{V}_h$ and a given $g \in L^1(\Omega)$, we introduce the discrete partial derivatives $\partial^{\pm}_{h,x_i}, \partial^{\pm,g}_{h,x_i} : \mathcal{V}_h \to V_h (i = 1, 2)$ as follows:

$$\left(\partial^{\pm}_{h,x_i} v, \varphi_h\right)_{\mathcal{T}_h} := \left\langle Q^{\pm}_i(v) n^{(i)}, [\varphi_h]\right\rangle_{\mathcal{E}_h} - \left(v, \partial_{x_i}\varphi_h\right)_{\mathcal{T}_h}, \tag{2.4a}$$

$$\left(\partial^{\pm,g}_{h,x_i} v, \varphi_h\right)_{\mathcal{T}_h} := \left\langle Q^{\pm}_i(v) n^{(i)}, [\varphi_h]\right\rangle_{\mathcal{E}^I_h} + \left\langle g n^{(i)}, \varphi_h\right\rangle_{\mathcal{E}^B_h} - \left(v, \partial_{x_i}\varphi_h\right)_{\mathcal{T}_h} \tag{2.4b}$$

for all $\varphi_h \in V_h$. Accordingly, for any $v \in \mathcal{V}_h$, the discrete gradient operators are defined as:

$$\nabla^{\pm}_h v = (\partial^{\pm}_{h,x_1} v, \partial^{\pm}_{h,x_2} v) \quad \text{and} \quad \nabla^{\pm}_{h,g} v = (\partial^{\pm,g}_{h,x_1} v, \partial^{\pm,g}_{h,x_2} v).$$

We define the average operators $\overline{\partial}_{h,x_i} v$, $\overline{\partial}^g_{h,x_i} v$, $\overline{\nabla}_h v$, and $\overline{\nabla}_{h,g} v$ as follows,

$$\overline{\partial}_{h,x_i} v := \frac{1}{2}(\partial^{+}_{h,x_i} v + \partial^{-}_{h,x_i} v), \qquad \overline{\partial}^g_{h,x_i} v := \frac{1}{2}(\partial^{+,g}_{h,x_i} v + \partial^{-,g}_{h,x_i} v),$$
$$\overline{\nabla}_h v := \frac{1}{2}(\nabla^{+}_h v + \nabla^{-}_h v), \qquad \overline{\nabla}_{h,g} v := \frac{1}{2}(\nabla^{+}_{h,g} v + \nabla^{-}_{h,g} v).$$

Similarly, we can also define the discrete divergence operators $\text{div}^{\pm}_h, \overline{\text{div}}_h : \mathcal{V}_h \to V_h$ as follows,

$$\text{div}^{\pm}_h \mathbf{v} = \sum_{i=1}^{2} \partial^{\pm}_{h,x_i} v^{(i)} \quad \text{and} \quad \overline{\text{div}}_h \mathbf{v} = \frac{1}{2}(\text{div}^{+}_h \mathbf{v} + \text{div}^{-}_h \mathbf{v}). \tag{2.5}$$

2.2. Preliminary properties

We present some preliminary properties of the DG operators defined in the previous subsection and some results that will be used in the subsequent analysis. We first need the following generalized integration by parts formula.

Lemma 2.1. *For any $v_h \in V_h$ and $\varphi_h \in V_h$, we have*

$$\begin{aligned}(\partial^{\pm}_{h,x_i}(\zeta_i v_h), \varphi_h)_{\mathcal{T}_h} &= -(\partial^{\mp}_{h,x_i}(\zeta_i \varphi_h), v_h)_{\mathcal{T}_h} + (\varphi_h, (\partial_{x_i}\zeta_i) v_h)_{\mathcal{T}_h} \\ &\quad + \langle \zeta_i \varphi_h, v_h n^{(i)}\rangle_{\mathcal{E}^B_h}.\end{aligned} \tag{2.6}$$

Proof. By the definitions of $\partial^{\pm}_{h,x_i}$, $Q^{\pm}_i$, the fact that $\zeta_i \in W^{1,\infty}(\Omega)$, and integration by parts, we have

$$\begin{aligned}(\partial^{\pm}_{h,x_i}(\zeta_i v_h), \varphi_h)_{\mathcal{T}_h} &= \langle Q^{\pm}_i(\zeta_i v_h) n^{(i)}, [\varphi_h]\rangle_{\mathcal{E}_h} - (\zeta_i v_h, \partial_{x_i}\varphi_h)_{\mathcal{T}_h} \\ &= \langle \zeta_i Q^{\pm}_i(v_h) n^{(i)}, [\varphi_h]\rangle_{\mathcal{E}_h} - (\zeta_i v_h, \partial_{x_i}\varphi_h)_{\mathcal{T}_h} \\ &= (\partial_{x_i}(\zeta_i v_h), \varphi_h)_{\mathcal{T}_h} + \langle \zeta_i (Q^{\pm}_i(v_h) - \{v_h\}), [\varphi_h] n^{(i)}\rangle_{\mathcal{E}_h} \\ &\quad - \langle \zeta_i [v_h], \{\varphi_h\} n^{(i)}\rangle_{\mathcal{E}^I_h} \\ &= (\partial_{x_i}(\zeta_i v_h), \varphi_h)_{\mathcal{T}_h} \pm \langle \frac{1}{2}\,\text{sgn}(n^{(i)})[v_h]\zeta_i, [\varphi_h] n^{(i)}\rangle_{\mathcal{E}^I_h} \\ &\quad - \langle \zeta_i [v_h], \{\varphi_h\} n^{(i)}\rangle_{\mathcal{E}^I_h} \\ &= (\partial_{x_i}(\zeta_i v_h), \varphi_h)_{\mathcal{T}_h} \\ &\quad + \langle \zeta_i [v_h], \pm\frac{1}{2}|n^{(i)}|[\varphi_h] n^{(i)} - \{\varphi_h\} n^{(i)}\rangle_{\mathcal{E}^I_h}.\end{aligned} \tag{2.7}$$

Use the definition of $\partial^{\pm}_{h,x_i}$ again, we have

$$\begin{aligned}(\zeta_i \varphi_h, \partial_{x_i} v_h)_{\mathcal{T}_h} &= -(\partial^{\mp}_{h,x_i}(\zeta_i \varphi_h), v_h)_{\mathcal{T}_h} + \langle \zeta_i Q^{\mp}_i(\varphi_h) n^{(i)}, [v_h]\rangle_{\mathcal{E}_h} \\ &= -(\partial^{\mp}_{h,x_i}(\zeta_i \varphi_h), v_h)_{\mathcal{T}_h} + \langle \zeta_i \{\varphi_h\}, [v_h] n^{(i)}\rangle_{\mathcal{E}^I_h} \\ &\quad \mp \langle \frac{1}{2}|n^{(i)}|[\varphi_h]\zeta_i, [v_h]\rangle_{\mathcal{E}^I_h} + \langle \zeta_i \varphi_h, v_h n^{(i)}\rangle_{\mathcal{E}^B_h}.\end{aligned} \tag{2.8}$$

Note that $(\partial_{x_i}(\zeta_i v_h), \varphi_h)_{\mathcal{T}_h} = (\zeta_i \varphi_h, \partial_{x_i} v_h)_{\mathcal{T}_h} + (\varphi_h, (\partial_{x_i}\zeta_i) v_h)_{\mathcal{T}_h}$. Insert (2.8) into (2.7), we have

$$\begin{aligned}(\partial^{\pm}_{h,x_i}(\zeta_i v_h), \varphi_h)_{\mathcal{T}_h} &= -(\partial^{\mp}_{h,x_i}(\zeta_i \varphi_h), v_h)_{\mathcal{T}_h} + (\varphi_h, (\partial_{x_i}\zeta_i) v_h)_{\mathcal{T}_h} \\ &\quad + \langle \zeta_i \varphi_h, v_h n^{(i)}\rangle_{\mathcal{E}^B_h}. \quad \square\end{aligned} \tag{2.9}$$

Remark 2.2. The immediate consequence of Lemma 2.1 is the following,

$$\begin{aligned}(\text{div}^{\pm}_h(\boldsymbol{\zeta} v_h), \varphi_h)_{\mathcal{T}_h} &= -(\text{div}^{\mp}_h(\boldsymbol{\zeta}\varphi_h), v_h)_{\mathcal{T}_h} + (\varphi_h, (\nabla\cdot\boldsymbol{\zeta}) v_h)_{\mathcal{T}_h} \\ &\quad + \langle \boldsymbol{\zeta}\cdot\mathbf{n}, v_h\varphi_h\rangle_{\mathcal{E}^B_h}.\end{aligned} \tag{2.10}$$

Remark 2.3. Another consequence of the derivation (2.7) is the following,

$$(\overline{\text{div}}_h(\boldsymbol{\zeta} v_h), \varphi_h)_{\mathcal{T}_h} = (\nabla\cdot(\boldsymbol{\zeta} v_h), \varphi_h)_{\mathcal{T}_h} - \langle \boldsymbol{\zeta}\cdot\mathbf{n}[v_h], \{\varphi_h\}\rangle_{\mathcal{E}^I_h}. \tag{2.11}$$

In fact, the following is also valid,

$$(\overline{\text{div}}_h(\boldsymbol{\zeta} v), \varphi_h)_{\mathcal{T}_h} = (\nabla\cdot(\boldsymbol{\zeta} v), \varphi_h)_{\mathcal{T}_h} \quad \forall v \in H^1(\Omega). \tag{2.12}$$

3. The reduced problem and discretization

Our goal is to design a numerical method based on the DG differential calculus framework for (1.1) (or (1.3)). Since the DWDG method for the diffusion part is well-established [21], we first consider the following reduced problem by taking $\varepsilon = 0$,

$$\nabla\cdot(\boldsymbol{\zeta} u^0) + (\gamma - \nabla\cdot\boldsymbol{\zeta}) u^0 = f \quad \text{in} \quad \Omega, \tag{3.1a}$$

$$u^0 = g \quad \text{on} \quad \partial\Omega^-, \tag{3.1b}$$

where the inflow part of the boundary Ω^- is defined as

$$\partial\Omega^- := \{x \in \partial\Omega : \boldsymbol{\zeta}(x)\cdot\mathbf{n}(x) < 0\}.$$

Here $\mathbf{n}$ is the outward unit normal vector of $\partial\Omega$ at x.

Let $V^0 := \{v \in L_2(\Omega) \mid \boldsymbol{\zeta}\cdot\nabla v \in L_2(\Omega)\}$. Then the weak form of the problem (3.1) is to find $u^0 \in V^0$ such that

$$a^{ar}(u^0, v) = (f, v)_{L_2(\Omega)} + \int_{\partial\Omega^-} |\boldsymbol{\zeta}\cdot\mathbf{n}| g\, v\, dx \quad \forall v \in V^0, \tag{3.2}$$

where the bilinear form $a^{ar}(\cdot,\cdot)$ is defined as

$$a^{ar}(v, w) = (\nabla\cdot(\boldsymbol{\zeta} v), w)_{L_2(\Omega)} + ((\gamma - \nabla\cdot\boldsymbol{\zeta}) v, w)_{L_2(\Omega)} + \int_{\partial\Omega^-} |\boldsymbol{\zeta}\cdot\mathbf{n}| v\, w\, dx. \tag{3.3}$$

The problem (3.2) is well-posed [7] under the assumption (1.2).

The discrete problem for (3.2) is to find $u^0_h \in V_h$ such that

$$a^{ar}_h(u^0_h, v_h) = (f, v_h)_{L_2(\Omega)} + \int_{\partial\Omega^-} |\boldsymbol{\zeta}\cdot\mathbf{n}| g\, v_h\, dx \quad \forall v_h \in V_h. \tag{3.4}$$

Here the bilinear form $a^{ar}_h(\cdot,\cdot)$ is defined as,

$$a^{ar}_h(v, w) = (\overline{\text{div}}_h(\boldsymbol{\zeta} v), w)_{\mathcal{T}_h} + ((\gamma - \nabla\cdot\boldsymbol{\zeta}) v, w)_{L_2(\Omega)} + \int_{\partial\Omega^-} |\boldsymbol{\zeta}\cdot\mathbf{n}| v\, w\, ds, \tag{3.5}$$

where $\overline{\text{div}}_h$ is defined in (2.5).

Remark 3.1. In (3.5), we approximate the divergence operator $\nabla\cdot$ with the discrete divergence operator $\overline{\text{div}}_h$ defined in (2.5).

3.1. Consistency

Let u^0 be the solution to (3.1) and u^0_h be the solution to (3.4). We have, by (2.12),

$$\begin{aligned} a_h^{ar}(u^0, v_h) &= (\overline{\mathrm{div}}_h(\zeta u^0), v_h)_{\mathcal{T}_h} + ((\gamma - \nabla\cdot\zeta)u^0, v_h)_{L_2(\Omega)} \\ &\quad + \int_{\partial\Omega^-} |\zeta\cdot\mathbf{n}| u^0\, v_h\, ds \\ &= (\nabla\cdot(\zeta u^0), v_h)_{\mathcal{T}_h} + ((\gamma - \nabla\cdot\zeta)u^0, v_h)_{L_2(\Omega)} \\ &\quad + \int_{\partial\Omega^-} |\zeta\cdot\mathbf{n}| u^0\, v_h\, ds \\ &= (\nabla\cdot(\zeta u^0) + (\gamma - \nabla\cdot\zeta)u^0, v_h)_{L_2(\Omega)} \\ &\quad + \int_{\partial\Omega^-} |\zeta\cdot\mathbf{n}| u^0\, v_h\, ds \\ &= (f, v_h)_{L_2(\Omega)} + \int_{\partial\Omega^-} |\zeta\cdot\mathbf{n}| g\, v_h\, ds \\ &= a_h^{ar}(u_h^0, v_h) \quad \forall v_h \in V_h. \end{aligned} \tag{3.6}$$

Therefore we have the usual Galerkin orthogonality

$$a_h^{ar}(u^0 - u_h^0, v_h) = 0 \quad \forall v_h \in V_h. \tag{3.7}$$

3.2. L_2 coercivity

Define the norm

$$\|v\|_{ar}^2 = \|v\|_{L_2(\Omega)}^2 + \int_{\partial\Omega} \frac{1}{2}|\zeta\cdot\mathbf{n}| v^2\, ds. \tag{3.8}$$

Lemma 3.2. *We have*

$$a_h^{ar}(v_h, v_h) \ge C\|v_h\|_{ar}^2 \quad \forall v_h \in V_h. \tag{3.9}$$

Proof. It follows from (2.10) that

$$\begin{aligned} a_h^{ar}(v_h, v_h) &= (\overline{\mathrm{div}}_h(\zeta v_h), v_h)_{\mathcal{T}_h} + ((\gamma - \nabla\cdot\zeta)v_h, v_h)_{L_2(\Omega)} \\ &\quad + \int_{\partial\Omega^-} |\zeta\cdot\mathbf{n}| v_h^2\, ds \\ &= \frac{1}{2}(\mathrm{div}_h^+(\zeta v_h), v_h)_{\mathcal{T}_h} + \frac{1}{2}(\mathrm{div}_h^-(\zeta v_h), v_h)_{\mathcal{T}_h} \\ &\quad + ((\gamma - \nabla\cdot\zeta)v_h, v_h)_{L_2(\Omega)} + \int_{\partial\Omega^-} |\zeta\cdot\mathbf{n}| v_h^2\, ds \\ &= \frac{1}{2}(v_h, (\nabla\cdot\zeta)v_h)_{\mathcal{T}_h} + \frac{1}{2}\langle \zeta\cdot\mathbf{n}, v_h^2\rangle_{\mathcal{E}_h^B} + \\ &\quad + ((\gamma - \nabla\cdot\zeta)v_h, v_h)_{L_2(\Omega)} + \int_{\partial\Omega^-} |\zeta\cdot\mathbf{n}| v_h^2\, ds \\ &= ((\gamma - \frac{1}{2}\nabla\cdot\zeta)v_h, v_h)_{L_2(\Omega)} + \int_{\partial\Omega} \frac{1}{2}|\zeta\cdot\mathbf{n}| v_h^2 ds. \end{aligned} \tag{3.10}$$

The estimate (3.9) immediately follows from the assumption (1.2). □

Remark 3.3. Using (2.11), we obtain

$$\begin{aligned} a_h^{ar}(u_h^0, v_h) &= (\nabla\cdot(\zeta u_h^0), v_h)_{\mathcal{T}_h} - \langle \zeta\cdot\mathbf{n}[u_h^0], \{v_h\}\rangle_{\mathcal{E}_h^I} \\ &\quad + ((\gamma - \nabla\cdot\zeta)u_h^0, v_h)_{L_2(\Omega)} + \int_{\partial\Omega^-} |\zeta\cdot\mathbf{n}| u_h^0\, v_h\, ds. \end{aligned} \tag{3.11}$$

Therefore, the proposed method (3.4) is consistent with the standard centered fluxes DG method (cf. [7]).

3.3. Stabilization

It is well-known that the solution to (3.11) (or equivalently, (3.4)) exhibits spurious oscillations near the outflow boundary if no additional stabilization is added. Hence, we define the following method with a stabilization term: Find $u_h^0 \in V_h$ such that

$$a_h^{upw}(u_h^0, v_h) = (f, v_h)_{L_2(\Omega)} + \int_{\partial\Omega^-} |\zeta\cdot\mathbf{n}| g\, v_h\, dx \quad \forall v_h \in V_h, \tag{3.12}$$

where the bilinear form $a_h^{upw}(\cdot,\cdot)$ is defined as,

$$a_h^{upw}(v, w) = a_h^{ar}(v, w) + \langle \frac{1}{2}|\zeta\cdot\mathbf{n}|[v], [w]\rangle_{\mathcal{E}_h^I}. \tag{3.13}$$

Remark 3.4. The method (3.12) can be interpreted as an upwind method [7].

It is trivial to see that (3.12) is a consistent method in the sense that

$$a_h^{upw}(u^0 - u_h^0, v_h) = 0 \quad \forall v_h \in V_h. \tag{3.14}$$

Define the norm $\|\cdot\|_{upw}$ on V_h as

$$\|v\|_{upw}^2 = \|v\|_{ar}^2 + \sum_{e\in\mathcal{E}_h^I} \int_e \frac{1}{2}|\zeta\cdot\mathbf{n}|[v]^2\, ds. \tag{3.15}$$

Lemma 3.5. *We have, for all $v \in V_h$,*

$$a_h^{upw}(v_h, v_h) \ge C\|v_h\|_{upw}^2. \tag{3.16}$$

Proof. The coercivity follows from (3.9), (3.13), and (3.15) immediately. □

3.4. Convergence analysis

We would like to establish the error estimates of the stabilized method (3.12). Note that (3.12) is well-posed due to the discrete coercivity (3.16). Note that the norm $\|\cdot\|_{upw}$ is not strong enough to establish a boundedness result for the bilinear form $a_h^{upw}(\cdot,\cdot)$ which is crucial to the convergence analysis. To remedy this issue, we define a stronger norm on $V^0 + V_h$,

$$\|v\|_{upw,*}^2 = \|v\|_{upw}^2 + \sum_{T\in\mathcal{T}_h} \|v\|_{L_2(\partial T)}^2. \tag{3.17}$$

We then have the following boundedness result (cf. [7, Lemma 2.30]).

Lemma 3.6. *We have, for all $v \in V^0$ and $w_h \in V_h$*

$$a_h^{upw}(v - \pi_h v, w_h) \le C\|v - \pi_h v\|_{upw,*}\|w_h\|_{upw}, \tag{3.18}$$

where $\pi_h : V^0 \to V_h$ is the L_2-orthogonal projection.

Proof. It follows from (3.11), (3.13) and integration by parts that

$$\begin{aligned} & a_h^{upw}(v - \pi_h v, w_h) \\ &= -(v - \pi_h v, \zeta\cdot\nabla w_h)_{\mathcal{T}_h} + \langle \zeta\cdot\mathbf{n}\{v - \pi_h v\}, [w_h]\rangle_{\mathcal{E}_h^I} \\ &\quad + ((\gamma - \nabla\cdot\zeta)(v - \pi_h v), w_h)_{L_2(\Omega)} + \int_{\partial\Omega^+} |\zeta\cdot\mathbf{n}|(v - \pi_h v)\, w_h\, ds \\ &\quad + \langle \frac{1}{2}|\zeta\cdot\mathbf{n}|[v - \pi_h v], [w_h]\rangle_{\mathcal{E}_h^I}. \end{aligned} \tag{3.19}$$

We have, by Cauchy-Schwarz inequality and (3.8),

$$\begin{aligned} & ((\gamma - \nabla\cdot\zeta)(v - \pi_h v), w_h)_{L_2(\Omega)} + \int_{\partial\Omega^+} |\zeta\cdot\mathbf{n}|(v - \pi_h v)\, w_h\, ds \\ &\le C\|v - \pi_h v\|_{ar}\|w_h\|_{ar} \le C\|v - \pi_h v\|_{upw}\|w_h\|_{upw}. \end{aligned} \tag{3.20}$$

Similarly, it follows from (3.15) that

$$\langle \frac{1}{2}|\zeta\cdot\mathbf{n}|[v-\pi_h v],[w_h]\rangle_{\mathcal{E}_h^I} \le \|v-\pi_h v\|_{upw}\|w_h\|_{upw}. \tag{3.21}$$

Let $\langle\zeta\rangle_T$ be the mean value of ζ over T. Notice that $\langle\zeta\rangle_T\cdot\nabla w_h$ is a constant and hence we have, by the definition of π_h,

$$(v-\pi_h v, \langle\zeta\rangle_T\cdot\nabla w_h)_{\mathcal{T}_h} = 0 \quad \forall\, w_h\in V_h. \tag{3.22}$$

Notice that we assume $\zeta\in[W^{1,\infty}(\Omega)]^2$, and, hence we have $\|\zeta-\langle\zeta\rangle_T\|_{L^\infty(T)}\lesssim h_T$.

Therefore, we obtain, by (3.22) and inverse inequalities,

$$\begin{aligned}&(v-\pi_h v,\zeta\cdot\nabla w_h)_{\mathcal{T}_h}\\ =&(v-\pi_h v,(\zeta-\langle\zeta\rangle_T)\cdot\nabla w_h)_{\mathcal{T}_h}\\ \le& C\|v-\pi_h v\|_{upw}\sum_{T\in\mathcal{T}_h} h_T\|\nabla w_h\|_{L_2(T)}\\ \le& C\|v-\pi_h v\|_{upw}\sum_{T\in\mathcal{T}_h}\|w_h\|_{L_2(T)}\\ \le& C\|v-\pi_h v\|_{upw}\|w_h\|_{upw}.\end{aligned} \tag{3.23}$$

Lastly, we have

$$\begin{aligned}&\langle\zeta\cdot\mathbf{n}\{v-\pi_h v\},[w_h]\rangle_{\mathcal{E}_h^I}\\ \le& C\sum_{T\in\mathcal{T}_h}\|v-\pi_h v\|^2_{L_2(\partial T)}\|w_h\|_{upw}\\ \le& C\|v-\pi_h v\|_{upw,*}\|w_h\|_{upw}.\end{aligned} \tag{3.24}$$

The estimate (3.18) follows from (3.19)-(3.24). □

Combining (3.14), (3.16), and (3.18), we conclude

$$\|u^0-u_h^0\|_{upw}\le C\|u^0-\pi_h u^0\|_{upw,*}. \tag{3.25}$$

By standard projection error estimates, we have (cf. [7]) the following theorem.

Theorem 3.7. *Let u^0 be the solution to (3.2) and u_h^0 be the solution to (3.12). Assume $u^0\in H^2(\Omega)$ and then we have*

$$\|u^0-u_h^0\|_{upw}\le Ch^{\frac{3}{2}}\|u^0\|_{H^2(\Omega)}. \tag{3.26}$$

3.5. Convergence analysis based on an inf-sup condition

We could obtain a similar error estimate with a stronger norm which involves the gradient in the direction of ζ. Define

$$\|v\|^2_{upw\sharp}=\|v\|^2_{upw}+\sum_{T\in\mathcal{T}_h}h_T\|\zeta\cdot\nabla v\|^2_{L_2(T)}. \tag{3.27}$$

We first need the following inf-sup condition (cf. [7]).

Lemma 3.8. *We have*

$$\sup_{w_h\in V_h\setminus\{0\}}\frac{a_h^{upw}(v_h,w_h)}{\|w_h\|_{upw\sharp}}\ge C\|v_h\|_{upw\sharp}\quad\forall v_h\in V_h, \tag{3.28}$$

where the constant C is independent of ζ and h.

Sketch of proof. The proof is identical to that of [7, Lemma 2.35] due to Remark 3.3. We briefly discuss the strategy here. Let $\mathcal{S}=\sup_{w_h\in V_h\setminus\{0\}}\frac{a_h^{upw}(v_h,w_h)}{\|w_h\|_{upw\sharp}}$. Given any $v_h\in V_h$, we construct a particular $w_h\in V_h\setminus\{0\}$ such that, for all $T\in\mathcal{T}_h$, $w_h|_T=h_T\langle\zeta\rangle_T\cdot\nabla v_h$, where $\langle\zeta\rangle_T$ denotes the mean value of ζ over T as in the proof of Lemma 3.6. We first notice that, by (3.16),

$$C\|v_h\|^2_{upw}\le a_h^{upw}(v_h,v_h)=\frac{a_h^{upw}(v_h,v_h)}{\|v_h\|_{upw\sharp}}\|v_h\|_{upw\sharp}\le\mathcal{S}\|v_h\|_{upw\sharp}. \tag{3.29}$$

We claim that

$$\sum_{T\in\mathcal{T}_h}h_T\|\zeta\cdot\nabla v_h\|^2_{L_2(T)}\lesssim\mathcal{S}\|v_h\|_{upw\sharp}+\|v_h\|_{upw}\|v_h\|_{upw\sharp}+\|v_h\|^2_{upw}. \tag{3.30}$$

Combining (3.30) and (3.16) and using (3.29) again, we have

$$C\|v_h\|^2_{upw\sharp}\lesssim\mathcal{S}\|v_h\|_{upw\sharp}+\|v_h\|_{upw}\|v_h\|_{upw\sharp}. \tag{3.31}$$

Upon using Young's inequality and iterating the inequality (3.29) once again, we have

$$C\|v_h\|^2_{upw\sharp}\lesssim\mathcal{S}\|v_h\|_{upw\sharp} \tag{3.32}$$

which leads to (3.28). The claimed estimate (3.30) can be proved by inverse inequalities, trace inequalities and the Cauchy-Schwarz inequality. For simplicity, we refer to [7, Lemma 2.35] for more details. □

To formulate a concrete error estimate, we define the following norm on V^0+V_h,

$$\|v\|^2_{upw\sharp,*}=\|v\|^2_{upw\sharp}+\sum_{T\in\mathcal{T}_h}(h_T^{-1}\|v\|^2_{L_2(T)}+\|v\|^2_{L_2(\partial T)}). \tag{3.33}$$

Similar to (3.18), we have (cf. [7]),

$$a_h^{upw}(v-\pi_h v,w_h)\le C\|v-\pi_h v\|_{upw\sharp,*}\|w_h\|_{upw\sharp} \tag{3.34}$$

for all $v\in V^0$ and $w_h\in V_h$.

The immediate consequence of (3.28) and (3.34) is the following lemma.

Lemma 3.9. *Let u^0 be the solution to (3.2) and u_h^0 be the solution to (3.12). Assume $u^0\in H^2(\Omega)$ and then we have*

$$\|u^0-u_h^0\|_{upw\sharp}\le C\|u^0-\pi_h u^0\|_{upw\sharp,*}\le Ch^{\frac{3}{2}}\|u^0\|_{H^2(\Omega)}. \tag{3.35}$$

Proof. It follows from (3.28), (3.34), and (3.14) that,

$$\begin{aligned}\|\pi_h u^0-u_h^0\|_{upw\sharp}&\le C\sup_{w_h\in V_h\setminus\{0\}}\frac{a_h^{upw}(\pi_h u^0-u_h^0,w_h)}{\|w_h\|_{upw\sharp}}\\ &=C\sup_{w_h\in V_h\setminus\{0\}}\frac{a_h^{upw}(\pi_h u^0-u^0,w_h)}{\|w_h\|_{upw\sharp}}\\ &\le C\|u^0-\pi_h u^0\|_{upw\sharp,*}.\end{aligned} \tag{3.36}$$

The first inequality in (3.35) is immediate due to triangle inequality and (3.36). For the second inequality, we have

$$\sum_{T\in\mathcal{T}_h}h_T\|\zeta\cdot\nabla(u^0-\pi_h u^0)\|^2_{L_2(T)}\le Ch^3\|u^0\|^2_{H^2(\Omega)} \tag{3.37}$$

and

$$\sum_{T\in\mathcal{T}_h}h_T^{-1}\|u^0-\pi_h u^0\|^2_{L_2(T)}\le Ch^3\|u^0\|^2_{H^2(\Omega)} \tag{3.38}$$

by standard projection error estimates. We finish the proof by combining Theorem 3.7, (3.27), (3.33), (3.37), and (3.38). □

4. The full problem and discretization

The weak form of the problem (1.3) is to find $u\in V_g:=\{v\in H^1(\Omega):v=g \text{ on } \partial\Omega\}$ such that

$$a(u,v)=(f,v)_{L_2(\Omega)}\quad\forall\, v\in H_0^1(\Omega), \tag{4.1}$$

where the bilinear form $a(\cdot,\cdot)$ is defined as

$$a(v,w)=\varepsilon a^d(v,w)+a^{ar}(v,w) \tag{4.2}$$

for the bilinear form $a^d(v,w) := (\nabla v, \nabla w)_{L_2(\Omega)}$ and $a^{ar}(\cdot,\cdot)$ defined in (3.3). The problem (4.1) is well-posed [7] under the assumption (1.2).

The discrete problem for (4.1) is to find $u_h \in V_h$ such that

$$a_h(u_h, v_h) = (f, v_h)_{L_2(\Omega)} + \int_{\partial\Omega^-} |\zeta\cdot\mathbf{n}| g\, v_h\, dx - \varepsilon\langle g, \overline{\nabla}_{h,0} v_h \cdot \mathbf{n} - \frac{\sigma_e}{h_e} v_h\rangle_{\mathcal{E}_h^B} \quad \forall v_h \in V_h, \tag{4.3}$$

where the bilinear form $a_h(\cdot,\cdot) := \varepsilon a_h^d(\cdot,\cdot) + a_h^{upw}(\cdot,\cdot)$. Here the bilinear form $a_h^{upw}(\cdot,\cdot)$ is defined in (3.13) and $a_h^d(\cdot,\cdot)$ (cf. [22]) is defined as

$$a_h^d(v,w) := \frac{1}{2}\left[(\nabla^+_{h,0} v, \nabla^+_{h,0} w)_{\mathcal{T}_h} + (\nabla^-_{h,0} v, \nabla^-_{h,0} w)_{\mathcal{T}_h}\right] + \langle \frac{\sigma_e}{h_e}[v],[w]\rangle_{\mathcal{E}_h} \tag{4.4}$$

with the penalty parameter $\sigma_e \ge 0$ for all $e \in \mathcal{E}_h$.

Remark 4.1. Unlike most standard DG methods where the penalty parameter is positive, DWDG methods allow $\sigma_e = 0$ for all $e \in \mathcal{E}_h$ under the assumptions $\mathcal{T}_h$ is locally quasi-uniform and each simplex in the triangulation has at most one boundary edge. This result was established in [21,22,10] for a diffusive equation. Here we maintain the same assumptions and allow the case where $\sigma_e = 0$ for the general convection-diffusion-reaction equation.

4.1. Consistency

Let u be the solution to (1.3) and u_h be the solution to (4.3). It follows from [22] and (3.14) that

$$a_h(u - u_h, v_h) = -\varepsilon\langle\{\overline{\nabla}_{h,g} u - \nabla u\}\cdot\mathbf{n}, [v_h]\rangle_{\mathcal{E}_h} \quad \forall v_h \in V_h. \tag{4.5}$$

Remark 4.2. The method (4.3) is not consistent in the sense of (4.5).

4.2. Coercivity

Define the norm $\|\cdot\|_h$ on V_h by

$$\|v\|_h^2 := \varepsilon\|v\|_d^2 + \|v\|_{upw}^2, \tag{4.6}$$

where $\|\cdot\|_{upw}$ is defined in (3.15) and $\|\cdot\|_d$ is defined as

$$\|v\|_d^2 := \frac{1}{2}(\|\nabla^+_{h,0} v\|^2_{L_2(\Omega)} + \|\nabla^-_{h,0} v\|^2_{L_2(\Omega)}) + \sum_{e\in\mathcal{E}_h}\frac{\sigma_e}{h_e}\|[v]\|^2_{L_2(e)}. \tag{4.7}$$

It follows from (3.16), (4.4), and (4.7) that

$$a_h(v_h, v_h) \ge C\|v_h\|_h^2 \quad \forall v_h \in V_h. \tag{4.8}$$

4.3. Convergence analysis

Note that (4.3) is well-posed due to the discrete coercivity (4.8). It is shown (cf. [22, (3.15)]) that for $\sigma_e \ge 0$,

$$a_h^d(v,w) \le \|v\|_d\|w\|_d \quad \forall v, w \in V + V_h. \tag{4.9}$$

Consequently, we have, by (3.18) and (4.9),

$$a_h(v - \pi_h v, w_h) \le C\|v - \pi_h v\|_{h,*}\|w_h\|_h \quad \forall v \in V,\ w_h \in V_h, \tag{4.10}$$

where the norm $\|\cdot\|_{h,*}$ is defined by

$$\|v\|_{h,*}^2 = \varepsilon\|v\|_d^2 + \|v\|^2_{upw,*}. \tag{4.11}$$

Here the operator $\pi_h : V \to V_h$ is the L_2-orthogonal projection.

Theorem 4.3. *Let u be the solution to (1.3) and u_h be the solution to (4.3). Assume $u \in H^2(\Omega)$ and then we have*

$$\|u - u_h\|_h \le C(\varepsilon^{\frac{1}{2}} h + h^{\frac{3}{2}})\|u\|_{H^2(\Omega)}. \tag{4.12}$$

Proof. It follows from [22, Theorem 4.2] and [7] that

$$\begin{aligned}\|u - \pi_h u\|_h^2 &= \varepsilon\|u - \pi_h u\|_d^2 + \|u - \pi_h u\|^2_{upw}\\ &\le C(\varepsilon h^2 + h^3)\|u\|^2_{H^2(\Omega)}.\end{aligned} \tag{4.13}$$

It follows from (4.8), (4.5), and (4.10) that

$$\begin{aligned}\|\pi_h u - u_h\|_h^2 &\lesssim a_h(\pi_h u - u_h, \pi_h u - u_h)\\ &= a_h(\pi_h u - u, \pi_h u - u_h) + a_h(u - u_h, \pi_h u - u_h)\\ &\lesssim \|u - \pi_h u\|_{h,*}\|\pi_h u - u_h\|_h\\ &\quad - \varepsilon\langle\{\overline{\nabla}_{h,g} u - \nabla u\}\cdot\mathbf{n}, [\pi_h u - u_h]\rangle_{\mathcal{E}_h}.\end{aligned} \tag{4.14}$$

It is shown in [22] that

$$\left|\langle\{\overline{\nabla}_{h,g} u - \nabla u\}\cdot\mathbf{n}, [\pi_h u - u_h]\rangle_{\mathcal{E}_h}\right| \le Ch\|u\|_{H^2(\Omega)}\|\pi_h u - u_h\|_d, \tag{4.15}$$

and hence

$$\varepsilon\left|\langle\{\overline{\nabla}_{h,g} u - \nabla u\}\cdot\mathbf{n}, [\pi_h u - u_h]\rangle_{\mathcal{E}_h}\right| \le C\varepsilon^{\frac{1}{2}} h\|u\|_{H^2(\Omega)}\|\pi_h u - u_h\|_h. \tag{4.16}$$

Similar to Theorem 3.7, we have, by the trace inequality with scaling,

$$\begin{aligned}\sum_{T\in\mathcal{T}_h}\|u - \pi_h u\|^2_{L_2(\partial T)} &\le C\sum_{T\in\mathcal{T}_h} h_T^{-1}\|u - \pi_h u\|^2_{L_2(T)}\\ &\quad + h_T\|\nabla(u - \pi_h u)\|^2_{L_2(T)}\\ &\le Ch^3\|u\|_{H^2(\Omega)}.\end{aligned} \tag{4.17}$$

It follows from (4.13), (4.11), and (3.17) that

$$\|u - \pi_h u\|_{h,*} \le C(\varepsilon^{\frac{1}{2}} h + h^{\frac{3}{2}})\|u\|_{H^2(\Omega)}. \tag{4.18}$$

We then conclude, by (4.18), (4.14), and (4.16),

$$\|\pi_h u - u_h\|_h \le C(\varepsilon^{\frac{1}{2}} h + h^{\frac{3}{2}})\|u\|_{H^2(\Omega)}. \tag{4.19}$$

Combining (4.13), (4.19), and triangle inequality, we obtain

$$\|u - u_h\|_h \le C(\varepsilon^{\frac{1}{2}} h + h^{\frac{3}{2}})\|u\|_{H^2(\Omega)}. \quad \square \tag{4.20}$$

4.4. Convergence analysis based on an inf-sup condition

We present an error estimate with a stronger norm that is similar to Section 3.5. Define

$$\|v\|^2_{h\sharp} = \|v\|_h^2 + \sum_{T\in\mathcal{T}_h} h_T\|\zeta\cdot\nabla v\|^2_{L_2(T)}. \tag{4.21}$$

We first need the following inf-sup condition (cf. [7, Lemma 2.35] and [13, Lemma A.1]).

Lemma 4.4. *We have*

$$\sup_{w_h\in V_h\setminus\{0\}}\frac{a_h(v_h, w_h)}{\|w_h\|_{h\sharp}} \ge C\|v_h\|_{h\sharp}. \tag{4.22}$$

Proof. We again follow the approaches in [7,8]. Let $\mathcal{S} = \sup_{w_h\in V_h\setminus\{0\}}\frac{a_h(v_h,w_h)}{\|w_h\|_{h\sharp}}$. Given any $v_h \in V_h$, we again construct a $w_h \in V_h\setminus\{0\}$ such that, for all $T \in \mathcal{T}_h$, $w_h|_T = h_T\langle\zeta\rangle_T\cdot\nabla v_h$. Similar to the proof of Lemma 3.8, we first notice that, by (4.8),

$$C\|v_h\|_h^2 \le a_h(v_h, v_h) = \frac{a_h(v_h, v_h)}{\|v_h\|_{h\sharp}}\|v_h\|_{h\sharp} \le \mathcal{S}\|v_h\|_{h\sharp}. \tag{4.23}$$

We claim that

$$\sum_{T\in\mathcal{T}_h} h_T\|\zeta\cdot\nabla v_h\|_{L_2(T)}^2 \lesssim S\|v_h\|_{h\sharp} + \|v_h\|_h\|v_h\|_{h\sharp} + \|v_h\|_h^2. \tag{4.24}$$

Combining (4.24) and (4.23) and using (4.23) again, we have

$$C\|v_h\|_{h\sharp}^2 \lesssim S\|v_h\|_{h\sharp} + \|v_h\|_h\|v_h\|_{h\sharp}. \tag{4.25}$$

Upon using Young's inequality and iterating the inequality (4.23) once again, we have

$$C\|v_h\|_{h\sharp}^2 \lesssim S\|v_h\|_{h\sharp} \tag{4.26}$$

which leads to (4.22). The rest of the proof is devoted to (4.24). We first prove the estimate

$$\|w_h\|_{h\sharp} \lesssim \|v_h\|_{h\sharp}. \tag{4.27}$$

Indeed, it follows from (4.21) that

$$\|w_h\|_{h\sharp}^2 = \varepsilon\|w_h\|_d^2 + \|w_h\|_{upw}^2 + \sum_{T\in\mathcal{T}_h} h_T\|\zeta\cdot\nabla w_h\|_{L_2(T)}^2. \tag{4.28}$$

A standard inverse inequality implies

$$\sum_{T\in\mathcal{T}_h} h_T\|\zeta\cdot\nabla w_h\|_{L_2(T)}^2 \lesssim \sum_{T\in\mathcal{T}_h} h_T^{-1}\|w_h\|_{L_2(T)}^2 \tag{4.29}$$

and, together with a trace inequality

$$\begin{aligned}\|w_h\|_{upw}^2 &= \|w_h\|_{L_2(\Omega)}^2 + \int_{\partial\Omega}\frac{1}{2}|\zeta\cdot\mathbf{n}|w_h^2\,ds \\ &\quad + \sum_{e\in\mathcal{E}_h^I}\int_e \frac{1}{2}|\zeta\cdot\mathbf{n}|[w_h]^2\,ds \\ &\lesssim \|v_h\|_{L_2(\Omega)}^2 + \sum_{T\in\mathcal{T}_h} h_T^{-1}\|w_h\|_{L_2(T)}^2.\end{aligned} \tag{4.30}$$

We also have $\|w_h\|_d^2 \lesssim \|v_h\|_d^2$. In fact, we have, if $\sigma_{min} := \min_{e\in\mathcal{E}_h}\sigma_e > 0$,

$$\sum_{e\in\mathcal{E}_h}\frac{\sigma_e}{h_e}\|[w_h]\|_{L_2(e)}^2 \le C\sum_{T\in\mathcal{T}_h}\|\nabla v_h\|_{L_2(T)}^2 \le C(1+\frac{1}{\sigma_{min}})\|v_h\|_d^2, \tag{4.31}$$

where we use a standard trace inequality and [22, Lemma 4.1]. It also follows from [22, Lemma 4.1] and a trace inequality that, for $\sigma_e \ge 0$,

$$\begin{aligned}&\frac{1}{2}(\|\nabla_{h,0}^+ w_h\|_{L_2(\Omega)}^2 + \|\nabla_{h,0}^- w_h\|_{L_2(\Omega)}^2) \\ &\lesssim \sum_{T\in\mathcal{T}_h}\|\nabla w_h\|_{L_2(T)}^2 + \sum_{e\in\mathcal{E}_h}\frac{1}{h_e}\|[w_h]\|_{L_2(e)}^2 \\ &\lesssim \|v_h\|_d^2.\end{aligned} \tag{4.32}$$

The estimates (4.31) and (4.32) then imply $\|w_h\|_d^2 \lesssim \|v_h\|_d^2$.

At last, it is known that (cf. [7])

$$\sum_{T\in\mathcal{T}_h} h_T^{-1}\|w_h\|_{L_2(T)}^2 \lesssim \|v_h\|_{h\sharp}^2. \tag{4.33}$$

The estimate (4.27) is immediate upon combining (4.29)-(4.33).

It follows from (4.4), (3.11), and (3.12) that

$$\begin{aligned}\sum_{T\in\mathcal{T}_h} h_T\|\zeta\cdot\nabla v_h\|_{L_2(T)}^2 &= a_h(v_h,w_h) - \varepsilon a_h^d(v_h,w_h) \\ &\quad + (\zeta\cdot\nabla v_h, h_T(\zeta-\langle\zeta\rangle_T)\cdot\nabla v_h)_{\mathcal{T}_h} \\ &\quad + \langle\zeta\cdot\mathbf{n}[v_h],\{w_h\}\rangle_{\mathcal{E}_h^I} - (\gamma v_h, w_h)_{L_2(\Omega)} \\ &\quad - \int_{\partial\Omega^-}|\zeta\cdot\mathbf{n}|v_h\,w_h\,ds - \langle\frac{1}{2}|\zeta\cdot\mathbf{n}|[v_h],[w_h]\rangle_{\mathcal{E}_h^I} \\ &= T_1 + T_2\cdots + T_7.\end{aligned} \tag{4.34}$$

For the first two terms, we have, by (4.27) and (4.9),

$$|T_1| = |\frac{a_h(v_h,w_h)}{\|w_h\|_{h\sharp}}|\|w_h\|_{h\sharp}| \le S\|w_h\|_{h\sharp} \lesssim S\|v_h\|_{h\sharp}, \tag{4.35}$$

$$|T_2| \lesssim \varepsilon^{\frac{1}{2}}\|v_h\|_d\varepsilon^{\frac{1}{2}}\|w_h\|_d \lesssim \|v_h\|_h\|v_h\|_{h\sharp}. \tag{4.36}$$

It follows from Cauchy-Schwarz inequality and (4.27) that

$$|T_5| + |T_6| + |T_7| \lesssim \|v_h\|_h\|w_h\|_{h\sharp} \lesssim \|v_h\|_h\|v_h\|_{h\sharp}. \tag{4.37}$$

To bound T_4, we have, by a standard trace inequality, (4.33), and (4.27),

$$\begin{aligned}&\langle\zeta\cdot\mathbf{n}[v_h],\{w_h\}\rangle_{\mathcal{E}_h^I} \\ &\le \left(\sum_{e\in\mathcal{E}_h^I}\int_e\frac{1}{2}|\zeta\cdot\mathbf{n}|[v_h]^2\,ds\right)^{\frac{1}{2}}\left(\sum_{e\in\mathcal{E}_h^I}\int_e 2|\zeta\cdot\mathbf{n}|\{w_h\}^2\,ds\right)^{\frac{1}{2}} \\ &\lesssim \|v_h\|_h\left(\sum_{T\in\mathcal{T}_h} h_T^{-1}\|w_h\|_{L_2(T)}^2\right)^{\frac{1}{2}} \lesssim \|v_h\|_h\|v_h\|_{h\sharp}.\end{aligned} \tag{4.38}$$

Finally, we bound T_3 as follows,

$$\begin{aligned}&(\zeta\cdot\nabla v_h, h_T(\zeta-\langle\zeta\rangle_T)\cdot\nabla v_h)_{\mathcal{T}_h} \\ &\quad\lesssim \left(\sum_{T\in\mathcal{T}_h} h_T\|\zeta\cdot\nabla v_h\|_{L_2(T)}^2\right)^{\frac{1}{2}}\left(\sum_{T\in\mathcal{T}_h} h_T\|v_h\|_{L_2(T)}^2\right)^{\frac{1}{2}} \\ &\quad\lesssim \left(\sum_{T\in\mathcal{T}_h} h_T\|\zeta\cdot\nabla v_h\|_{L_2(T)}^2\right)^{\frac{1}{2}}\|v_h\|_{h\sharp} \\ &\quad\lesssim \frac{1}{2}\sum_{T\in\mathcal{T}_h} h_T\|\zeta\cdot\nabla v_h\|_{L_2(T)}^2 + C\|v_h\|_{h\sharp}^2,\end{aligned} \tag{4.39}$$

where we use an inverse inequality and Young's inequality. We also use the fact $\zeta \in [W^{1,\infty}(\Omega)]^2$, and, hence, $\|\zeta-\langle\zeta\rangle_T\|_{L^\infty(T)} \lesssim h_T$. The claimed estimate (4.24) follows from (4.34)-(4.39). ☐

Similar to Section 3.5, we define the following norm on $V + V_h$,

$$\|v\|_{h\sharp,*}^2 := \|v\|_{h\sharp}^2 + \sum_{T\in\mathcal{T}_h}(h_T^{-1}\|v\|_{L_2(T)}^2 + \|v\|_{L_2(\partial T)}^2). \tag{4.40}$$

We then have (cf. [7])

$$a_h(v-\pi_h v, w_h) \le C\|v-\pi_h v\|_{h\sharp,*}\|w_h\|_{h\sharp}, \tag{4.41}$$

for all $v \in V$ and $w_h \in V_h$. We omit the proof here since it is similar to that of Lemma 3.18.

Consequently, we obtain the following convergence theorem from (4.22) and (4.41).

Theorem 4.5. *Let u be the solution to (1.3) and u_h be the solution to (4.3). Assume $u \in H^2(\Omega)$ and then we have*

$$\|u-u_h\|_{h\sharp} \le C(\varepsilon^{\frac{1}{2}}h + h^{\frac{3}{2}})\|u\|_{H^2(\Omega)}. \tag{4.42}$$

Proof. It follows from (4.5), (4.22), (4.41), and (4.16) that

$$\begin{aligned}\|\pi_h u - u_h\|_{h\sharp} &\le C\sup_{w_h\in V_h\setminus\{0\}}\frac{a_h(\pi_h u - u_h, w_h)}{\|w_h\|_{h\sharp}} \\ &= C\sup_{w_h\in V_h\setminus\{0\}}\frac{a_h(\pi_h u - u, w_h) + a_h(u-u_h,w_h)}{\|w_h\|_{h\sharp}} \\ &\le C\|u-\pi_h u\|_{h\sharp,*} + C\varepsilon^{\frac{1}{2}}h\|u\|_{H^2(\Omega)}.\end{aligned} \tag{4.43}$$

We also obtain the following estimate, by (4.18) and arguments similar to (3.37) and (3.38),

$$\|u-\pi_h u\|_{h\sharp,*} \le C(\varepsilon^{\frac{1}{2}}h + h^{\frac{3}{2}})\|u\|_{H^2(\Omega)}. \tag{4.44}$$

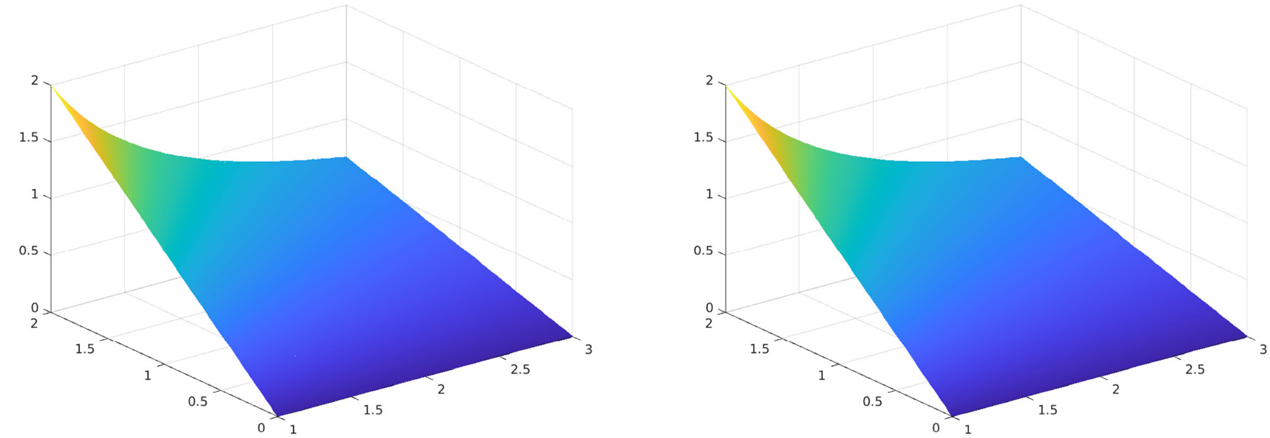

Fig. 2. Results of Example 5.1: u_h (left) and u (right) for $h = 1/128$.

We finish the proof by combining (4.43), (4.44), and triangle inequality. □

Remark 4.6. Theorem 4.5 implies the following convergence results,

$$\|u - u_h\|_{h\sharp} \leq \begin{cases} O(h) & \text{when (1.3) is diffusion-dominated,} \\ O(h^{\frac{3}{2}}) & \text{when (1.3) is convection-dominated.} \end{cases} \tag{4.45}$$

Note that $\|u\|_{H^2(\Omega)} = O(\varepsilon^{-\frac{3}{2}})$ ([30, Part III, Lemma 1.18]), hence, the estimate (4.42) is not informative when $\varepsilon \leq h$. More delicate interior error estimates that stay away from the boundary layers and interior layers for standard DG methods can be found in [24,15].

5. Numerical results

In this section, we present some numerical examples that support the theoretical results. All experiments are performed using MATLAB. We measure the absolute errors both globally and locally to examine the convergence behaviors of our numerical methods. For comparison, we test the penalty parameter choices $\sigma_e = 5$ and $\sigma_e = 0$ for all $e \in \mathcal{E}_h$. Note that our primary focus is on the convection-dominated scenario where ε is small. Consequently, the penalty parameter σ_e has a minimal impact, as demonstrated by the following numerical results.

Example 5.1 *(Smooth solution).* In this example, we take $\Omega = [1,3] \times [0,2]$, $\gamma = 2$, $\zeta = [x_1, x_2]^t$, and $\varepsilon = 10^{-9}$. We define the exact solution as

$$u(x_1, x_2) = \frac{x_2}{x_1}. \tag{5.1}$$

We show the global convergence rates in Table 1. We observe $O(h^2)$ convergence in the L_2 norm and $O(h^{\frac{3}{2}})$ convergence in the $\|\cdot\|_h$ and $\|\cdot\|_{h\sharp}$ norms. See Fig. 2 for an illustration of the numerical solution and the exact solution. Note that the convergence rates are all optimal. Indeed, the optimal convergence rates in L^2 norm is due to the smoothness of the solution, similar convergence behavior was observed in [1]. The optimal convergence rates in the $\|\cdot\|_h$ and $\|\cdot\|_{h\sharp}$ norms match with our theoretical results in Remark 4.6.

Example 5.2 *(Boundary layer [1]).* In this example, we take $\Omega = [0,1]^2$, $\gamma = 0$, $\zeta = [1,1]^t$, and $\varepsilon = 10^{-9}$. We define the exact solution as

$$u(x_1, x_2) = x_1 + x_2(1 - x_1) + \frac{e^{-1/\varepsilon} - e^{\frac{(x_1-1)(1-x_2)}{\varepsilon}}}{1 - e^{-1/\varepsilon}}. \tag{5.2}$$

Note that the exact solution exhibits boundary layers near $x_1 = 1$ and $x_2 = 1$.

Table 1
Errors and rates of convergence for u_h on $\Omega = [1,3] \times [0,2]$ for Example 5.1 when $\varepsilon = 10^{-9}$.

		L_2		$\|\cdot\|_h$		$\|\cdot\|_{h\sharp}$	
	h	Error	Rate	Error	Rate	Error	Rate
$\sigma_e = 0$	1/4	6.86e-03	-	2.99e-02	-	5.66e-02	-
	1/8	1.95e-03	1.81	1.08e-02	1.47	2.09e-02	1.43
	1/16	5.31e-04	1.88	3.84e-03	1.49	7.57e-03	1.47
	1/32	1.39e-04	1.93	1.36e-03	1.50	2.70e-03	1.49
	1/64	3.57e-05	1.96	4.81e-04	1.50	9.61e-04	1.49
$\sigma_e = 5$	1/4	6.86e-03	-	2.99e-02	-	5.66e-02	-
	1/8	1.95e-03	1.81	1.08e-02	1.47	2.09e-02	1.43
	1/16	5.31e-04	1.88	3.84e-03	1.49	7.57e-03	1.47
	1/32	1.39e-04	1.93	1.36e-03	1.50	2.70e-03	1.49
	1/64	3.57e-05	1.96	4.81e-04	1.50	9.61e-04	1.49

Table 2
Errors and rates of convergence for Example 5.2 on the subdomain $[0, 0.875]^2$ (away from the boundary layer) when $\varepsilon = 10^{-9}$.

		L_2		$\|\cdot\|_h$		$\|\cdot\|_{h\sharp}$	
	h	Error	Rate	Error	Rate	Error	Rate
$\sigma_e = 0$	1/8	2.32e-04	–	2.29e-03	–	2.10e-02	–
	1/16	5.81e-05	2.00	8.08e-04	1.50	7.43e-03	1.50
	1/32	1.45e-05	2.00	2.85e-04	1.50	2.63e-03	1.50
	1/64	3.63e-06	2.00	1.00e-04	1.50	9.28e-04	1.50
$\sigma_e = 5$	1/8	2.32e-04	–	2.29e-03	–	2.10e-02	–
	1/16	5.81e-05	2.00	8.08e-04	1.50	7.43e-03	1.50
	1/32	1.45e-05	2.00	2.85e-04	1.50	2.63e-03	1.50
	1/64	3.63e-06	1.99	1.00e-04	1.50	9.28e-04	1.50

As observed in Fig. 3, the numerical solution u_h has no spurious oscillations in the convection-dominated regime. It is also obvious that the numerical solution u_h ignores the boundary layers since we impose boundary conditions weakly.

Table 2 shows the local convergence results on the subdomain $[0, 0.875]^2$ in the L_2 norm, the $\|\cdot\|_h$ norm and the $\|\cdot\|_{h\sharp}$ norm. We observe $O(h^{\frac{3}{2}})$ convergence in the $\|\cdot\|_h$ and $\|\cdot\|_{h\sharp}$ norms as well as $O(h^2)$ convergence in the L_2 norm. Note that the local convergence behavior in the L_2 norm is optimal which indicates the boundary layer does not pollute the solution in the interior.

In Table 3, we show the global errors in the L_2 norm, the $\|\cdot\|_h$ norm and the $\|\cdot\|_{h\sharp}$ norm on $\Omega = [0,1]^2$. We observe again the optimal convergence in the L_2 norm. Notice that the global $\|\cdot\|_h$ errors do not converge at all due to the sharp boundary layer near the outflow boundary. Similar convergence behaviors were also observed in [1].

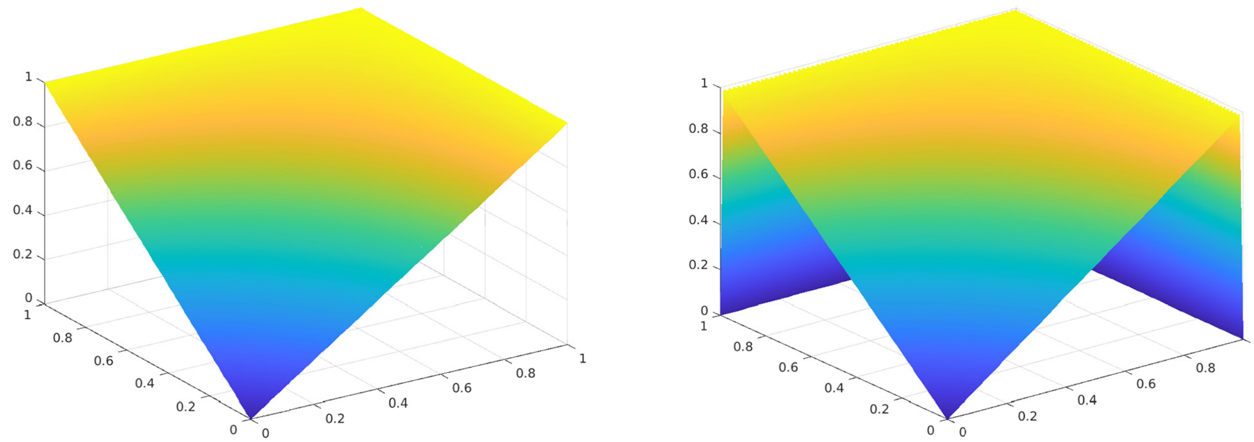

Fig. 3. Results of Example 5.2: u_h (left) and u (right) for $\varepsilon = 10^{-9}$, $h = {}^{1}/_{128}$.

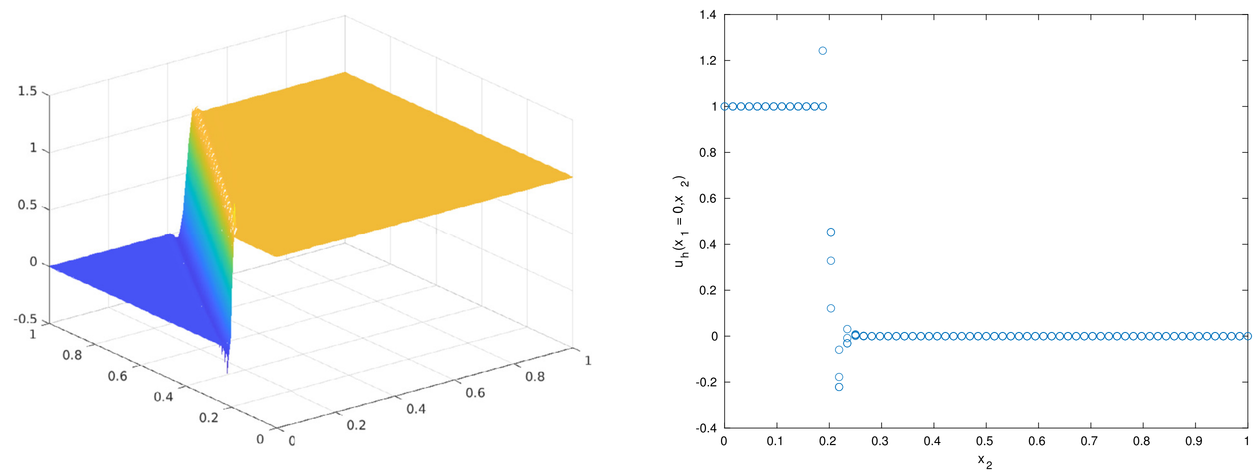

Fig. 4. Results of Example 5.3: u_h (left) and the profile of u_h at $x_1 = 0$ (right) for $\varepsilon = 10^{-9}$ and $h = {}^{1}/_{128}$.

Table 3
Errors and rates of convergence for u_h on $\Omega = [0,1]^2$ for Example 5.2 when $\varepsilon = 10^{-9}$.

		L_2		$\|\|\cdot\|\|_h$		$\|\|\cdot\|\|_{h\sharp}$	
	h	Error	Rate	Error	Rate	Error	Rate
$\sigma_e = 0$	1/4	1.06e-03	-	1.00e+00	-	1.00e+00	-
	1/8	2.66e-04	2.00	1.00e+00	0.00	1.00e+00	0.00
	1/16	6.64e-05	2.00	1.00e+00	0.00	1.00e+00	0.00
	1/32	1.66e-05	2.00	1.00e+00	0.00	1.00e+00	0.00
	1/64	4.15e-06	2.00	1.00e+00	0.00	1.00e+00	0.00
$\sigma_e = 5$	1/4	1.06e-03	-	1.00e+00	-	1.00e+00	-
	1/8	2.66e-04	1.99	1.00e+00	0.00	1.00e+00	0.00
	1/16	6.64e-05	2.00	1.00e+00	0.00	1.00e+00	0.00
	1/32	1.66e-05	2.00	1.00e+00	0.00	1.00e+00	0.00
	1/64	4.15e-06	2.00	1.00e+00	0.00	1.00e+00	0.00

Example 5.3 *(Interior layer [1]).* In this example, we take $\Omega = [0,1]^2$, $\gamma = 0$, $\zeta = [\frac{1}{2}, \frac{\sqrt{3}}{2}]^t$, $f = 0$, and the Dirichlet boundary conditions as:

$$u(x_1,x_2) = \begin{cases} 1, & \text{on } \{x_2 = 0, 0 \le x_1 \le 1\}, \\ 1, & \text{on } \{x_1 = 0, x_2 \le \frac{1}{5}\}, \\ 0, & \text{elsewhere.} \end{cases}$$

Fig. 4 shows that the presence of an internal layer in the approximate solution. Although the internal layer is captured by the approximate solution, there is small overshooting/undershooting along the internal layer. This is emphasized in the picture on the right in Fig. 4 where the profile of u_h is plotted on $\{x_1 : x_1 = 0\} \times \{x_2 : x_2 \in [0,1]\}$. For comparison, we show the numerical solution for $\varepsilon = 10^{-3}$ in Fig. 5. The behavior of our numerical methods is similar to standard DG methods (cf. [1]). For example, there are wiggles near the outflow boundary in the intermediate regime and the boundary layer is ignored on the outflow boundary.

Example 5.4 *(Interior layer [24]).* In this example, we take $\Omega = [0,1]^2$, $\gamma = 0$, $\zeta = [1,0]^t$, and $\varepsilon = 10^{-9}$. The exact solution is

$$u(x_1,x_2) = (1-x_1)^3 \arctan\left(\frac{x_2 - 0.5}{\varepsilon}\right). \tag{5.3}$$

As one can see from Fig. 6, the exact solution u has an internal layer along $x_2 = 0.5$. It is also clear that the numerical solution does not resolve the interior layer (cf. [24]).

In Table 4, we compute the local convergence in the L_2 norm, the $\|\cdot\|_h$ norm and the $\|\cdot\|_{h\sharp}$ norm. We again observe $O(h^2)$ convergence in the L_2 norm and $O(h^{\frac{3}{2}})$ convergence in the $\|\cdot\|_h$ and $\|\cdot\|_h\sharp$ norms. One can see that the convergence rates are optimal in the region where the solution is smooth. This indicates that the interior layer does not pollute the solution into the region that stays away from the interior layer.

For comparison, we show the global convergence rates in Table 5. We see that the convergence rates deteriorate when h is small due to the interior layer. We also illustrate the behavior of our numerical methods

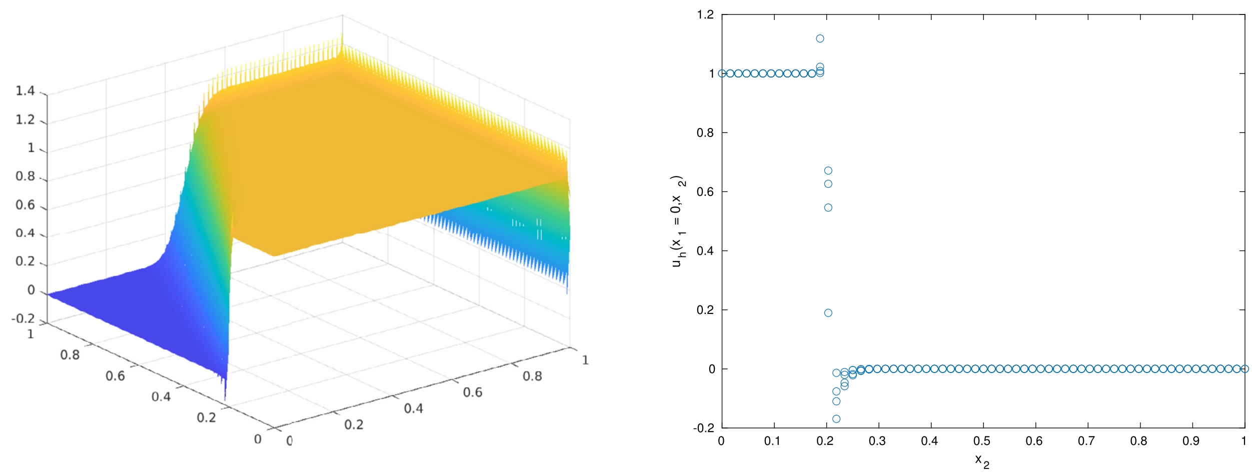

Fig. 5. Results of Example 5.3: u_h (left) and the profile of u_h at $x_1 = 0$ (right) for $\varepsilon = 10^{-3}$ and $h = 1/128$.

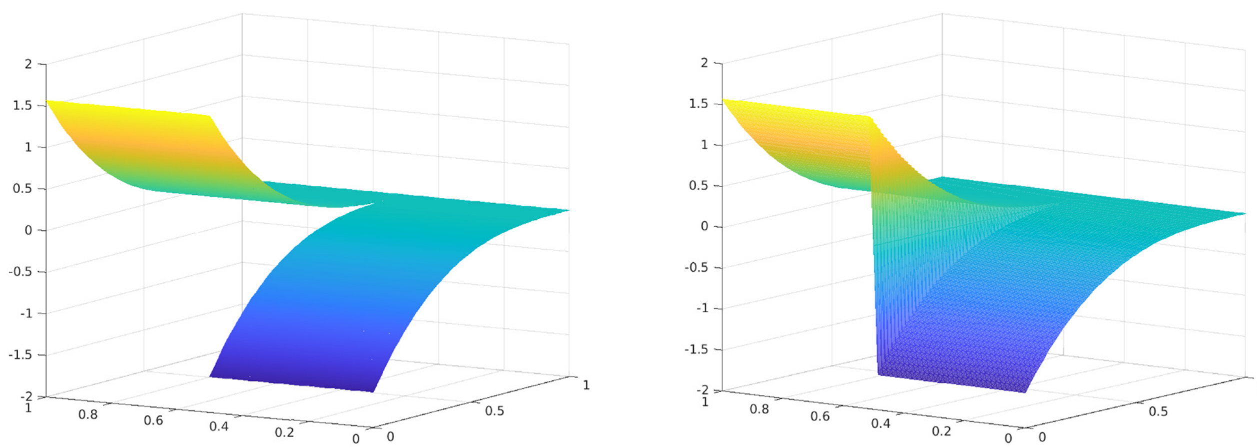

Fig. 6. Results of Example 5.4: u_h (left) and u (right) for $\varepsilon = 10^{-9}$ and $h = 1/128$.

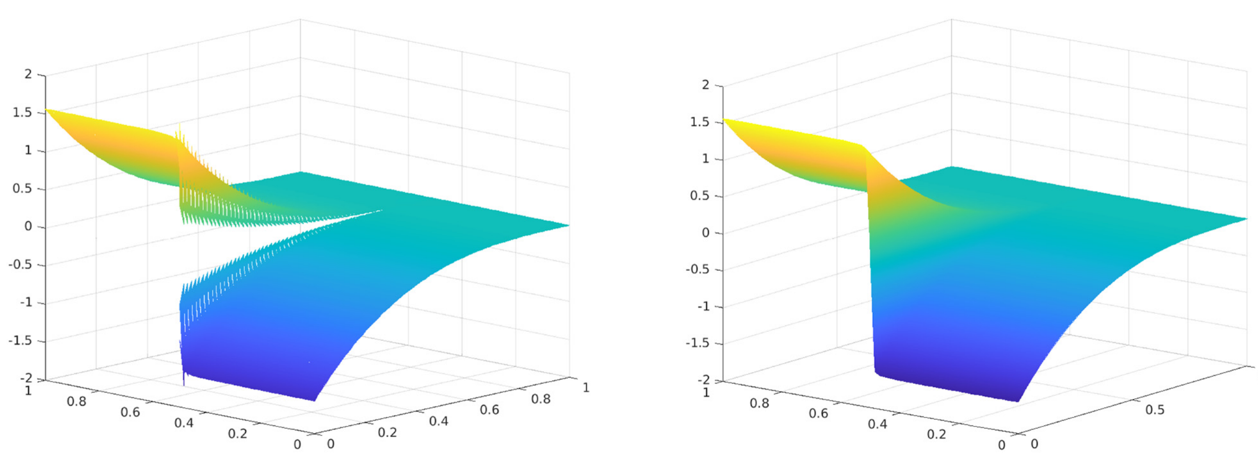

Fig. 7. Results of Example 5.4: u_h (left) and u (right) for $\varepsilon = 10^{-3}$ and $h = 1/128$.

in Figs. 7 and 8 when $\varepsilon = 10^{-3}$ and $\varepsilon = 1$. We can clearly see our methods capture the interior layer when ε increases.

6. Concluding remarks

In this paper we developed and analyzed numerical approximations based on the DG finite element differential calculus framework for a convection-diffusion-reaction equation. We proved that the proposed methods have optimal convergence behaviors, in the sense of Remark 4.6, in the convection-dominated regime. As a byproduct, we also showed that the method for the reduced convection-reaction problem is equivalent to a centered fluxes DG method. Numerically, we also observed that our methods have optimal convergence rates in the interior of the domain which are away from the boundary layers and interior layers. An interesting problem is to extend our methods to an optimal control problem that is constrained by a convection-dominated equation (cf. [27,26]). This is being investigated in an ongoing project.

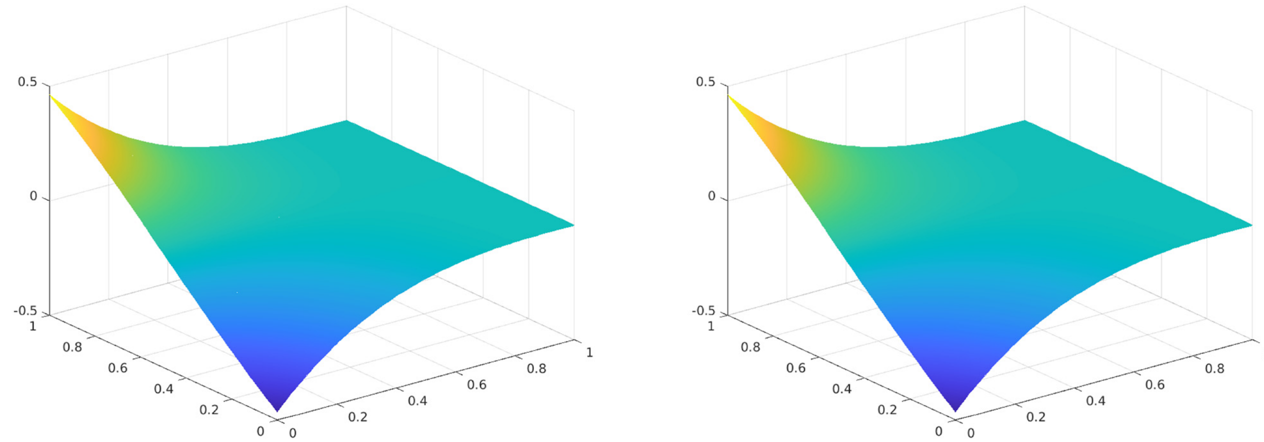

Fig. 8. Results of Example 5.4: u_h (left) and u (right) for $\varepsilon = 1$ and $h = 1/128$.

Table 4
Errors and rates of convergence for u_h for Example 5.4 in the subdomain $[0,1]\times[0.625,1]$ (away from the interior layer) when $\varepsilon = 10^{-9}$.

		L_2		$\|\|\cdot\|\|_h$		$\|\|\cdot\|\|_{h\sharp}$	
	h	Error	Rate	Error	Rate	Error	Rate
$\sigma_e = 0$	1/8	9.57e-04	–	8.16e-03	–	5.78e-02	–
	1/16	2.42e-04	1.98	2.88e-03	1.50	2.04e-02	1.49
	1/32	6.10e-05	1.99	1.02e-03	1.50	7.23e-03	1.50
	1/64	1.53e-05	2.00	3.59e-04	1.50	2.55e-03	1.50
$\sigma_e = 5$	1/8	9.57e-04	–	8.16e-03	–	5.78e-02	–
	1/16	2.42e-04	1.98	2.88e-03	1.50	2.04e-02	1.49
	1/32	6.10e-05	1.99	1.02e-03	1.50	7.23e-03	1.50
	1/64	1.53e-05	2.00	3.59e-04	1.50	2.55e-03	1.50

Table 5
Errors and rates of convergence for Example 5.4 on $\Omega = [0,1]^2$ for $\varepsilon = 10^{-9}$.

		L_2		$\|\|\cdot\|\|_h$		$\|\|\cdot\|\|_{h\sharp}$	
	h	Error	Rate	Error	Rate	Error	Rate
$\sigma_e = 0$	1/4	6.06e-03	-	3.77e-02	-	1.00e-01	-
	1/8	1.56e-04	1.96	1.33e-02	1.50	3.56e-02	1.50
	1/16	3.96e-04	1.98	4.73e-03	1.49	1.26e-02	1.50
	1/32	9.97e-05	1.99	1.82e-03	1.38	4.51e-03	1.48
	1/64	2.72e-05	1.87	1.19e-03	0.60	1.89e-03	1.26
$\sigma_e = 5$	1/4	6.06e-03	-	3.77e-02	-	1.00e-01	-
	1/8	1.56e-04	1.96	1.33e-02	1.50	3.56e-02	1.50
	1/16	3.96e-04	1.98	4.74e-03	1.49	1.26e-02	1.50
	1/32	9.97e-05	1.99	1.88e-03	1.33	4.53e-03	1.47
	1/64	2.95e-05	1.76	1.37e-03	0.45	2.00e-03	1.18

Data availability

Data will be made available on request.

Acknowledgement

This material is based upon work supported by the National Science Foundation under Grants No. DMS-2111059, DMS-2111004, and DMS-1929284 while the third author was in residence at the Institute for Computational and Experimental Research in Mathematics in Providence, RI, during the “Numerical PDEs: Analysis, Algorithms, and Data Challenges” program.

References

[1] B. Ayuso, L.D. Marini, Discontinuous Galerkin methods for advection-diffusion-reaction problems, SIAM J. Numer. Anal. 47 (2) (2009) 1391–1420.
[2] S.B. Boyana, T. Lewis, A. Rapp, Y. Zhang, Convergence analysis of a symmetric dual-wind discontinuous Galerkin method for a parabolic variational inequality, J. Comput. Appl. Math. 422 (2023) 114922.
[3] S.C. Brenner, L.R. Scott, The Mathematical Theory of Finite Element Methods, vol. 15, Springer Science & Business Media, 2008.
[4] F. Brezzi, L.D. Marini, E. Süli, Discontinuous Galerkin methods for first-order hyperbolic problems, Math. Models Methods Appl. Sci. 14 (12) (2004) 1893–1903.
[5] A.N. Brooks, T.J.R. Hughes, Streamline upwind/Petrov-Galerkin formulations for convection dominated flows with particular emphasis on the incompressible Navier-Stokes equations, Comput. Methods Appl. Mech. Eng. 32 (1–3) (1982) 199–259.
[6] P.G. Ciarlet, The Finite Element Method for Elliptic Problems, vol. 19, 1978.
[7] D.A. Di Pietro, A. Ern, Mathematical Aspects of Discontinuous Galerkin Methods, vol. 69, Springer Science & Business Media, 2011.
[8] A. Ern, J.-L. Guermond, Discontinuous Galerkin methods for Friedrichs’ systems. I. General theory, SIAM J. Numer. Anal. 44 (2) (2006) 753–778.
[9] P. Farrell, A. Hegarty, J.M. Miller, E. O’Riordan, G.I. Shishkin, Robust Computational Techniques for Boundary Layers, Chapman and Hall/CRC, 2000.
[10] X. Feng, T. Lewis, M. Neilan, Discontinuous Galerkin finite element differential calculus and applications to numerical solutions of linear and nonlinear partial differential equations, J. Comput. Appl. Math. 299 (2016) 68–91.
[11] X. Feng, T. Lewis, A. Rapp, Dual-wind discontinuous Galerkin methods for stationary Hamilton-Jacobi equations and regularized Hamilton-Jacobi equations, Commun. Appl. Math. Comput. 4 (2) (2022) 563–596.
[12] G. Fu, W. Qiu, W. Zhang, An analysis of HDG methods for convection-dominated diffusion problems, ESAIM: Math. Model. Numer. Anal. 49 (1) (2015) 225–256.
[13] J. Gopalakrishnan, G. Kanschat, A multilevel discontinuous Galerkin method, Numer. Math. 95 (2003) 527–550.
[14] J.-L. Guermond, Stabilization of Galerkin approximations of transport equations by subgrid modeling, ESAIM: Math. Model. Numer. Anal. 33 (6) (1999) 1293–1316.
[15] J. Guzmán, Local analysis of discontinuous Galerkin methods applied to singularly perturbed problems, J. Numer. Math. 14 (2006).
[16] T.J.R. Hughes, M. Mallet, M. Akira, A new finite element formulation for computational fluid dynamics: II. Beyond SUPG, Comput. Methods Appl. Mech. Eng. 54 (3) (1986) 341–355.
[17] C. Johnson, Numerical Solution of Partial Differential Equations by the Finite Element Method, Courier Corporation, 2012.
[18] H. Kim, J. Xu, L. Zikatanov, A multigrid method based on graph matching for convection–diffusion equations, Numer. Linear Algebra Appl. 10 (1–2) (2003) 181–195.
[19] P. Knobloch, A generalization of the local projection stabilization for convection-diffusion-reaction equations, SIAM J. Numer. Anal. 48 (2) (2010) 659–680.
[20] P. Knobloch, G. Lube, Local projection stabilization for advection–diffusion–reaction problems: one-level vs. two-level approach, Appl. Numer. Math. 59 (12) (2009) 2891–2907.
[21] T. Lewis, M. Neilan, Convergence analysis of a symmetric dual-wind discontinuous Galerkin method: convergence analysis of DWDG, J. Sci. Comput. 59 (2014) 602–625.
[22] T. Lewis, A. Rapp, Y. Zhang, Convergence analysis of symmetric dual-wind discontinuous Galerkin approximation methods for the obstacle problem, J. Math. Anal. Appl. 485 (2) (2020) 123840.
[23] T. Lewis, A. Rapp, Y. Zhang, Consistency results for the dual-wind discontinuous Galerkin method, J. Comput. Appl. Math. 431 (2023) 115257.

[24] D. Leykekhman, M. Heinkenschloss, Local error analysis of discontinuous Galerkin methods for advection-dominated elliptic linear-quadratic optimal control problems, SIAM J. Numer. Anal. 50 (4) (2012) 2012–2038.
[25] R. Lin, X. Ye, S. Zhang, P. Zhu, A weak Galerkin finite element method for singularly perturbed convection-diffusion–reaction problems, SIAM J. Numer. Anal. 56 (3) (2018) 1482–1497.
[26] S. Liu, Robust multigrid methods for discontinuous Galerkin discretizations of an elliptic optimal control problem, Comput. Methods Appl. Math. (2024).
[27] S. Liu, Z. Tan, Y. Zhang, Discontinuous Galerkin methods for an elliptic optimal control problem with a general state equation and pointwise state constraints, J. Comput. Appl. Math. 437 (2024) 115494.
[28] J. Miller, E. O'riordan, G.I. Shishkin, Fitted Numerical Methods for Singular Perturbation Problems: Error Estimates in the Maximum Norm for Linear Problems in One and Two Dimensions, World Scientific, 1996.
[29] K.W. Morton, Numerical Solution of Convection-Diffusion Problems, Applied Mathematics, Springer, Netherlands, 1995.
[30] H.-G. Roos, M. Stynes, L. Tobiska, Robust numerical methods for singularly perturbed differential equations, in: Convection-Diffusion-Reaction and Flow Problems, second edition, in: Springer Series in Computational Mathematics, vol. 24, Springer-Verlag, Berlin, 2008.
[31] M. Stynes, Steady-state convection-diffusion problems, Acta Numer. 14 (2005) 445–508.
[32] F. Wang, J. Xu, A crosswind block iterative method for convection-dominated problems, SIAM J. Sci. Comput. 21 (2) (1999) 620–645.
[33] J. Xu, L. Zikatanov, A monotone finite element scheme for convection-diffusion equations, Math. Comput. 68 (228) (1999) 1429–1446.